Advances in Science and Technology Research Journal

Advances in Science and Technology Research Journal, 2026, 20(5), 521–534
https://doi.org/10.12913/22998624/217367
ISSN 2299-8624, License CC-BY 4.0

Received: 2025.12.27
Accepted: 2026.03.15
Published: 2026.04.01

Path planning optimization of automated guided vehicles based on enhanced A* and dynamic window approach fusion algorithms

Zicheng Zhu[1,2], Qunzhang Tu[1], Xinmin Shen[1*], Qin Yin[1], Jiaojiao Zhang[1*], Shuwei Zhao[1], Jingguo Chen[1]

[1] Army Engineering University of PLA, Field Engineering College, No. 88 Houbiaoying Road, Nanjing, P.R. China
[2] China Heavy Duty Truck Group Co., Shunhua Road, Shandong, China
* Corresponding author's e-mail: xmshen2014@aeu.edu.cn, zjj1984@nuaa.edu.cn

ABSTRACT

Reasonable and efficient path is the key for the automated guided vehicle (AGV) to complete autonomous navigation transportation. The study aimed at the existing problems of the conventional A* path planning methods, such as the unsmooth path planning, vulnerability to local optimal, poor safety and stability. To address these issues, this research presented a novel path planning algorithm based on the fusion of enhanced A* algorithm and enhanced DWA. By introducing weight factors through an evaluation function and using the cubic B-spline curves, the search speed and path smoothness of A* algorithm were enhanced. The DWA algorithm was used to provide accurate directional guidance for automatic guided transport vehicles in local path planning, and the AGV obstacle avoidance ability in dynamic environments was enhanced by improving its evaluation function and weight fuzzy control. An enhanced algorithm was integrated to achieve the optimal global path and real-time obstacle avoidance function. Simulation experiment outcomes indicate that the enhanced A* algorithm achieves an average reduction of approximately 1.82% in path length and 61.24% in execution time. For instance, when tested on a 30 × 30 map, this method achieves a 4.45% reduction in path length, a 6.12% decrease in execution time, a 70.3% reduction in the count of turning points, and a 74.93% minimization of cumulative turning angles. Subsequently, the practicality and validity of the algorithm were further confirmed through real vehicle testing.

Keywords: path planning, automatic guided vehicle, enhanced A* algorithm, enhanced dynamic window algorithm, fusion algorithm.

INTRODUCTION

As industrial automation and artificial intelligence have advanced by leaps and bounds, the automated guided vehicle (AGV) has been widely used in the various fields, which greatly facilitates production and life of people, and also makes AGV become a research hot spot. The path planning is a key problem in the research field of AGV, and its purpose is to find an optimal path from the starting point to the target point for AGV [1].

Efficient and feasible operation path is the premise for AGV to complete various tasks independently. The path planning of AGV can be divided into static global path planning and dynamic local path planning [2–4] according to the complexity of scene environment and road conditions. At present, the commonly used global path planning algorithms mainly include A* algorithm [5], Dijkstra algorithm[6], particle swarm optimization algorithm and ant colony algorithm [7], as well as the local path planning algorithms mainly involve the dynamic window algorithm (DWA), artificial potential field algorithm (APF), and fuzzy logic algorithm [8–11]. On the basis of predictive control theory as well as acceleration and velocity constraints[12], DWA can plan a safe and smooth path in complex environment, and is often utilized in the robot local path planning [13]. However, the conventional A* algorithm often exhibits issues such as an excessive number of turning points and inadequate path smoothness. The conventional

DWA can easily fall into the trap and has the problem of local optimal solution [14–15]. To address the shortcomings of these conventional algorithms, the relevant scholars have studied and improved them. Li et al. optimized the A* algorithm through evaluation function, sub-node selection mode and path smoothness, which enhanced the path smoothness, but the search efficiency should be improved [16]. Wei et al. integrated the weight coefficients into the heuristic function of the A* algorithm to improve the selection strategy of the key point[17], and used the second-order Bezier curve to smooth the path trajectory to solve the problems of inefficiency and unsmooth path of the conventional A* algorithm [8]. Daniela et al. proposed a robot trajectory planner based on the P-DWA algorithm. This approach evaluates the running time and motion feasibility, and selects the optimal path [18]. Lai et al. put forward a fusion algorithm combining multi-scale map A * algorithm and improved DWA algorithm to enhance the flexibility of the path planning, but it was not verified by experimental verification [19].

Beyond algorithmic improvements, the performance of AGV navigation and path planning is significantly influenced by the capabilities and limitations of onboard sensors. Sensor systems such as LiDAR, cameras, and ultrasonic sensors provide essential environmental perception for localization, mapping, and obstacle detection. However, factors such as sensor noise, limited field of view, range constraints, and susceptibility to environmental interference directly impact the accuracy and reliability of path planning decisions, especially in dynamic and unstructured environments [20]. In dense obstacle fields or under high-speed motion, sensor latency and data association challenges can hinder timely obstacle avoidance. Moreover, sensor fusion strategies and the robustness of perception algorithms against uncertainties are critical for ensuring safe AGV operation. These sensor-related constraints underscore the importance of developing path planning algorithms that are not only computationally efficient, but also resilient to perceptual inaccuracies and can integrate predictive models to anticipate dynamic obstacle behavior [21].

In order to realize that AGV not only can run on the global optimal path, but also avoid obstacles in real time according to the environment, this research presents a novel path planning approach that integrates an enhanced A* algorithm with an enhanced DWA method. Firstly, the heuristic function of the conventional A* was adjusted to enhance the efficiency and safety of the path search by using the weight factor, and the cubic B-spline curve processing was applied to smooth the generated trajectory, ensuring a more stable movement. Secondly, based on the conventional DWA algorithm, the kinematics model of the AGV was established, and the robustness and stability of the algorithm were enhanced by increasing the distance correction function and weight fuzzy control. Finally, these two enhanced algorithms were fused, and the feasibility as well as validity of the combined algorithm were validated through simulation experiments and on-vehicle trials.

MATERIALS AND METHODS

Enhanced A* algorithm

As a heuristic search-based method, the A* algorithm integrates the strengths of Dijkstra algorithm and breadth-first search (BFS) algorithm [22]. It can find an optimal route while improving the efficiency of heuristic search. Therefore, this approach has gained extensive application in the field of intelligent vehicle navigation. The A* algorithm mainly utilizes the evaluation function to evaluate the cost value to guide the path search direction, and the evaluation function is expressed in Equation 1.

$$F(n) = G(n) + H(n) \tag{1}$$

where: $F(n)$ is the cost assessment of AGV from the initial node to the destination node, $G(n)$ is the real-world distance or effort AGV has already traveled from the starting node to its current node n, $H(n)$ is the estimated cost of AGV from the current node to the destination node.

In practical applications, the performance of the A* algorithm can vary significantly depending on the heuristic function selected, making it crucial to carefully select an appropriate heuristic function for optimal operation. At present, three frequently used heuristic functions exist, which include Manhattan distance, Chebyshev distance and Euclidean distance [23], and they are shown in Equations 2, 3 and 4 respectively.

$$H_{\mathrm{md}} = |x_1 - x_2| + |y_1 - y_2| \tag{2}$$

$$H_{\mathrm{cd}} = \max\left\{|x_1 - x_2|, |y_1 - y_2|\right\} \tag{3}$$

$$H_{ed} = \sqrt{(x_1 - x_2)^2 + (y_1 - y_2)^2} \quad (4)$$

As shown in Equations 2 to 4, the starting point is defined by the coordinates (x_1, y_1), while the target point has coordinates (x_2, y_2).

Although the conventional A* algorithm has excellent performance in navigating paths, it also has some limitations. Firstly, its performance is highly sensitive to the heuristic function, and an ill-designed heuristic may reduce the search efficiency or prevent finding the optimal solution. Secondly, the process of seeking the optimal path demands storing a significant volume of node data, and the large-scale space search requires huge memory consumption, which may exceed the limit of the system resource. Thirdly, it does not perform well in dynamic environments where changes in the environment may cause a searched path to fail.

Enhanced of algorithm evaluation function

It can be seen from Equation 1 that the choice of the heuristic function H(n) in the conventional A* algorithm plays a crucial role in determining both the search performance and the quality of the resulting path. In order to ensure that AGV can obtain the efficient and optimal path in the practical applications, the heuristic function H(n) was enhanced in this research. The heuristic function H(n) currently employed in this context relies on Euclidean distance, which inherently results in its computed value being consistently lower than the actual distance between the current node and the target node. In the scenarios where the current node is significantly distant from the target, the computed value of the heuristic function H(n) tends to be notably smaller than the true distance, leading to the algorithm encountering issues such as excessive node expansion and reduced computational performance. In such scenarios, the weight assigned to the heuristic function H(n) should be elevated to enhance the searching performance of the algorithm. As the algorithm approaches the target node, the heuristic function H(n) tends to approach the actual value it should have. To prevent the issue where the optimal path is not found because the heuristic function H(n) takes an excessively high value, the weight associated with this function must be decreased. To address this issue, the heuristic function undergoes adjustment by incorporating a weight factor, which was illustrated in Equation 5.

$$w = 1 + a \cdot \left(\frac{r}{R} \right) \quad (5)$$

where: r is the separation between the present node n and the target point, R is the distance from the initial point to the target position, and a is the fixed weight value.

Equation 6 presents the assessment metric utilized by the enhanced A* algorithm.

$$F(n) = G(n) + w \cdot H(n) \quad (6)$$

where: $F(n)$ is comprehensive cost value of the AGV, $G(n)$ is actual cost incurred by the AGV traveling from the initial node to the present node, $H(n)$ is the estimated cost of the AGV from the current node to the destination node, and w is weight factor.

By dynamically adjusting the weight factor w, the evaluation function can more accurately reflect the path length from the current node to the destination node. Especially when there are obstacles or terrain changes on the path, this adjustment helps to avoid overestimating or underestimating the path length, thereby enhancing the accuracy of path planning. Because the weight factor w considers the ratio of the overall distance from the origin to the destination to the distance from the current node to the destination, it serves to minimize the reliance on the algorithm on Euclidean distance metrics, thereby reducing the misleading caused by the straight line. Through estimating the path length more accurately, the enhanced evaluation function cuts down on unnecessary exploration, contributing to a higher level of search proficiency.

The admissibility of the heuristic function is a core prerequisite for the A* algorithm to achieve global optimal path search, with its key criterion being: the estimated value of the heuristic function H(n) must always be less than or equal to the true path cost h*(n) from the current node n to the target node, $H(n) \leq h^*(n)$. To address the optimization needs of the conventional A* algorithm, the enhanced A*algorithm proposed in this study improves the original heuristic function H(n) by introducing a dynamic weight factor w, forming the adjusted heuristic function in the form of w×H(n). To strictly ensure that this improved heuristic function still meets the admissibility requirement, explicit constraints are imposed on key parameters in the algorithm design: the fixed weight value a is limited to the interval $0 < a \leq 1$

to guarantee the rationality of weight adjustment. Meanwhile, during the path search process, the distance r from the current node n to the target node is inevitably shorter than or equal to the total distance R from the start node to the target node ($r \leq R$), from which it can be derived that the weight factor $w = a \times (r/R)$ ranges from $0 < w \leq 1$. On the basis of the aforementioned parameter constraints, the improved heuristic function $w \times H(n)$ satisfies $w \times H(n) \leq H(n)$. Combined with the inherent property of the original heuristic function H(n) that $H(n) \leq h^*(n)$, it can be further deduced that $w \times H(n) \leq h^*(n)$, thus maintaining the admissibility of the heuristic function. This design ensures that while the enhanced A* algorithm improves search efficiency and path smoothness, it can still stably find the global optimal path, which is highly consistent with the core theoretical characteristics of the original A* algorithm.

Enhanced path smoothing

While adjusting the heuristic function H(n) through the weight parameter w can enhance the algorithm performance, the resulting paths still exhibit excessive direction changes and poor continuity, which is not conducive to the smoothness of the driving and turning of AGV. Thus, path smoothing becomes an essential step in addressing this issue. At present, the commonly used path smooth methods are mainly the B-spline curve method and the Bezier curve method. The B-spline curve method connects control points by the interpolation to produce a smooth curve, which not only continues the advantages of Bezier curve method, but also makes up for its shortcomings. Because the cubic B-spline curve has two control points, it can be more flexible to adjust the shape of the curve to fit a smooth curve, so this study opts for cubic B-spline curves to handle the path planning of AGV. Locations F_i (i = 0, 1, …, n) of (n+1) points are determined from the path, and the Bezier curve with order (n+1) can be constructed, as shown in Equation 7.

$$P(t) = \sum_{i=0}^{n} P_i F_{i,k}(t) \tag{7}$$

where: P_i is curve control point, i is index value of the control points, and k is order of the B-spline basis function (with $0 \leq t \leq 1$)[24].

For cubic B-spline curves, the basis function is defined as Equation 8.

$$F_{i,k}(t) = \frac{1}{k!}\sum_{m=0}^{k-i}(-1)^m C_{k+1}^{m}(t+k-m-j)^k \tag{8}$$

If k is selected as 3 in the Equation 8, the cubic B-spline interpolation basis function can be obtained, as shown in Equation 9.

$$\begin{cases} F_{0,3}(t) = -\frac{1}{6}t^3 + \frac{1}{2}t^2 - \frac{1}{2}t + \frac{1}{6} \\ F_{1,3}(t) = \frac{1}{2}t^3 - t^2 + \frac{2}{3} \\ F_{2,3}(t) = -\frac{1}{2}t^3 + \frac{1}{2}t^2 + \frac{1}{2}t + \frac{1}{6} \\ F_{3,3}(t) = \frac{1}{6}t^3 \end{cases} \tag{9}$$

Thus, the cubic B-spline curve is represented by Equation 10.

$$F_{i,3}(t) = \begin{bmatrix} t^3 & t^2 & t & 1 \end{bmatrix} \begin{bmatrix} -\frac{1}{6} & \frac{1}{2} & -\frac{1}{2} & \frac{1}{6} \\ \frac{1}{2} & -1 & \frac{1}{2} & 0 \\ -\frac{1}{2} & 0 & \frac{1}{2} & 0 \\ \frac{1}{6} & \frac{2}{3} & \frac{1}{6} & 0 \end{bmatrix} \begin{bmatrix} F_i \\ F_{i+1} \\ F_{i+2} \\ F_{i+3} \end{bmatrix} \tag{10}$$

It can be seen from Equation 10 that the construction of a cubic B-spline curve relies on the use of 4 discrete points for the curve fitting, as shown in Figure 1. P_0 to P_3 are the four control points required by the spline curve to define the basic shape of the curve. M_1 and M_2 are the middle characteristic points on the spline curve to adjust the characteristic parameters of the curve (such as the tangent direction or curvature). S and E represent the initial and terminal positions of the generated curve respectively. If there are multiple segments, multi-segment fitting can be carried out, and the overall route presents a smooth appearance finally.

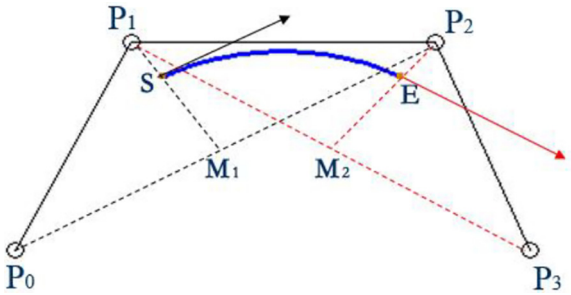

Figure 1. Multi-segment fitting of cubic B-spline curves

Enhanced DWA algorithm

In order to enhance the capability of AGV to avoid dynamic obstacles during its movement, the local dynamic planning algorithm is introduced based on the overall static path planning. On the basis of the preliminary research and combined with the running efficiency of the dynamic algorithm, this research selected DWA as the dynamic planning algorithm in this study. By dividing the moving space into various window and selecting the best window according to the current path environment and its status, the AGV can move safely and efficiently.

Kinematic model of AGV

In the environment of the production workshop, the AGV runs in a two-dimensional plane, so it has three degrees of freedom in the horizontal (X-axis),vertical (Y-axis) and turning angle directions. The motion model of AGV is shown in Figure 2. As depicted in Figure 2, assuming that AGV moves from time t_1 to time t_2,the movement distance and time are extremely short, the motion equation of AGV at these two times can be expressed by Equation 11.

$$\begin{cases} x(t_2) = x(t_1) + v\Delta t \cos(\theta(t_1)) \\ y(t_2) = y(t_1) + v\Delta t \sin(\theta(t_1)) \\ \theta(t_2) = \theta(t_1) + \omega\Delta t \end{cases} \quad (11)$$

where: $(x(t_1))$ and $(x(t_2))$ are the positions of the AGV at time t_1 and time t_2 respectively, $\theta(t_1)$ and $\theta(t_2)$ are the turning angle of the AGV at time t_1 and time t_2, v is the operating speed, and ω is the angular velocity of the AGV[25].

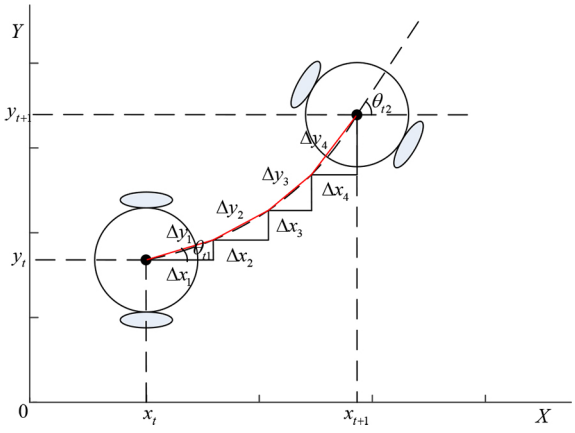

Figure 2. AGV kinematic model

Velocity sampling and evaluation function

According to the running situation of AGV, DWA needs to consider the current running speed and the possible speed changes when interacting with obstacles, and select the optimal running path in real time. Thus, considering the environment and dynamic constraints of AGV, it is important to achieve a safe and efficient path planning within the reasonable speed range.

Firstly, the running speed of AGV shall be controlled within the optimum range of angular and linear motion parameters[26],and the constraints for the range of operating speed are expressed in the Equation 12.

$$v_s = \left\{(v,\omega) \middle| v_{\min} \le v \le v_{\max}, \omega_{\min} \le \omega \le \omega_{\max}\right\} \quad (12)$$

where: v_{min} is the minimum operating linear velocity, v_{max} is maximum operating linear velocity, ω_{min} is minimum operating angular velocity, and ω_{max} is the maximum angular velocity[27].

Secondly, to guarantee AGV arrives at the target location smoothly, it is necessary to prevent collision through reasonably limiting the speed space of the transport vehicle when planning the local path and the environmental constraint is illustrated in Equation 13.

$$v_a = \left\{(v,\omega) \middle| v \le \sqrt{2dist(v,\omega)v_{\max}}, \omega \le \sqrt{2dist(v,\omega)\omega_{\max}}\right\} \quad (13)$$

where: dist(v, ω) is simulating the distance between the terminal of the track and the closest obstacle for the AGV.

Thirdly, due to the constraints imposed by the operational capabilities of the motor, AGV cannot exceed a certain threshold for acceleration, so the dynamic constraint is defined in Equation 14.

$$v_b = \left\{(v,\omega) \middle| v \in \left[v_1 - v_{\max}\Box t,\ v_1 + v_{\max}\Box t\right], \omega \in \left[\omega_1 - w_{\max}\Box t,\ \omega_1 + w_{\max}\Box t\right]\right\} \quad (14)$$

where: v_1 is the current linear velocity, ω_1 is current angular velocity, v_{max} is maximum operating linear velocity, and ω_{max} is maximum angular velocity for AGV [21]. The resulting final velocity sampling space can be represented in Equation 15.

$$v = v_s \bigcap v_a \bigcap v_b \quad (15)$$

In the speed sampling space, the multiple sets of operating trajectories can be collected, and different running tracks can plan different paths. The evaluation function can evaluate various paths, so that AGV can select optimal path with high efficiency. The evaluation function selected in this study is presented in Equation 16.

$$G(v,w) = \partial\left(\alpha Head(v,w) + \right.$$
$$\left. + \beta Dist(v,w) + \gamma Vel(v,w)\right) \quad (16)$$

where: head(v, w) is the heading angle evaluation function used to assess the degree to which the heading angle of the end position point of the simulated trajectory is oriented towards the target position, $Dist(v, w)$ is the obstacle avoidance safety evaluation function used to reflect the safety of the trajectory, $Vel(v, w)$ is the speed evaluation function used to assess the efficiency of AGV movement on simulated trajectories. α, β, γ are the weighting coefficients, and ∂ is the normalized processing parameters. The normalization of aforementioned evaluation functions is conducive to satisfy the optimal path selection.

Enhancement of evaluation function and weight fuzzy control

To enhance the robustness of the DWA algorithm while ensuring short runtime, fewer iterations, and a smooth path—with the goal of enabling AGV to complete autonomous obstacle avoidance tasks in real environments, this study increased the correction function of the distance $D_1ist(v, w)$ to optimize and enhance the evaluation function of the conventional DWA algorithm. The optimized and enhanced assessment metric is presented in Equation 17.

$$\partial\left(\alpha Head(v,w) + \beta Dist(v,w) + \right.$$
$$\left. + \gamma Vel(v,w) + \lambda D_1ist(v,w)\right) \quad (17)$$

When the weights are set in a fixed manner, the conventional DWA algorithm tends to become trapped in local optimal solutions when dealing with complex and ever-changing environments. This not only decreases the efficiency of path planning but also causes issues like oscillations or stagnation in the movement process. This issue manifests itself in two primary ways. Firstly, the adaptability of fixed weights is poor, especially in narrow passages, dense obstacles and other scenarios. Fixed obstacle avoidance weights may result in the excessive conservative and frequent deceleration or too aggressive approach to obstacles. Secondly, the response of dynamic environment is insufficient, when the environment changes due to moving obstacles, the static weight is difficult to adjust the strategy quickly, which impairs the real-time path optimization capability. To enhance the adaptability and optimization-seeking ability of DWA, a fuzzy controller is introduced to perform real-time adaptive adjustment of the weights of the evaluation function. The fuzzy control rules are shown in Table 1.

The fuzzy sets $\{N_1, N_2, N_3, N_4\}$ of the input variables in the Table 1 correspond to very near, near, moderate, and far distances, respectively. The fuzzy sets of the output variables in the table are $\{M_1, M_2, M_3, M_4\}$ corresponding to very small, small, medium and large weights respectively. Considering rule 4 in Table 1, for example, when AGV is close to obstacle and at a moderate distance from the target location, the strategy of giving up tracking the global and target points and completing the obstacle avoidance task first should be adopted to ensure the safety of the running line. According to the output rules in the table, the heading weight α is set to a small, the safety β is set to the maximum value, the speed weight γ is set to a medium, and the distance correction weight λ is set to a small. The output membership functions are presented in Figure 3.

Enhanced A* and enhanced DWA fusion algorithm

Despite its ability to generate a globally optimal path, the enhanced A* algorithm neglects the dynamic constraints intrinsic to AGV, thereby creating a gap between the path designed in the planning phase and the path executed during actual AGV operation. The enhanced DWA takes the final target point as the only reference, which easily leads the algorithm fall into local optimal solution, resulting in the failure of normal path planning and the failure to reach the target point. In view of the advantages and disadvantages of the above-mentioned two algorithms, the enhanced A* algorithm and the enhanced DWA algorithm are fused. In order to achieve the aforementioned integration, the subsequent process is followed. Firstly, the enhanced A * algorithm is used for global planning of AGV to obtain the optimal path sequence, and then the DWA algorithm is used for path planning at local

Table 1. Fuzzy control rules

No.	Input		Output			
	D_obs	D_goal	α	β	γ	λ
1	N_1	N_1	M_1	M_2	M_3	M_2
2	N_1	N_2	M_1	M_3	M_3	M_2
3	N_1	N_4	M_1	M_4	M_4	M_2
4	N_1	N_3	M_1	M_4	M_3	M_2
5	N_2	N_1	M_3	M_1	M_3	M_3
6	N_2	N_2	M_3	M_2	M_3	M_3
7	N_2	N_3	M_2	M	M_3	M_3
8	N_2	N_4	M_2	M_4	M_4	M_3
9	N_3	N_1	M_3	M_1	M_3	M_1
10	N_3	N_2	M_3	M_1	M_3	M_2
11	N_3	N_3	M_3	M_1	M_3	M_3
12	N_3	N_4	M_3	M_1	M_4	M_4
13	N_4	N_1	M_4	M_1	M_2	M_1
14	N_4	N_2	M_4	M_1	M_2	M_1
15	N_4	N_3	M_4	M_1	M_3	M_2

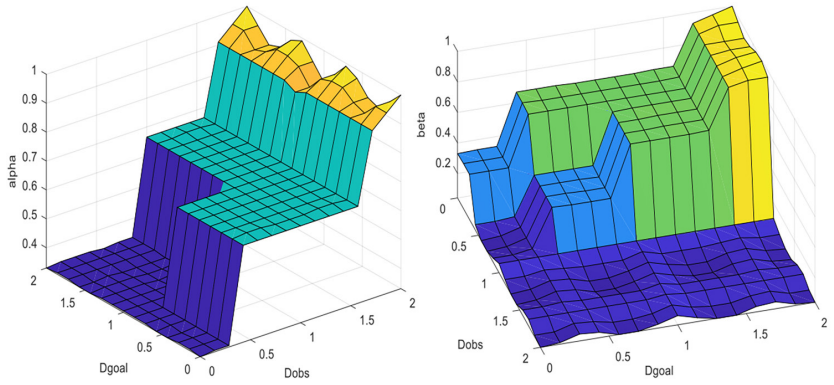

(a) α output (b) β output

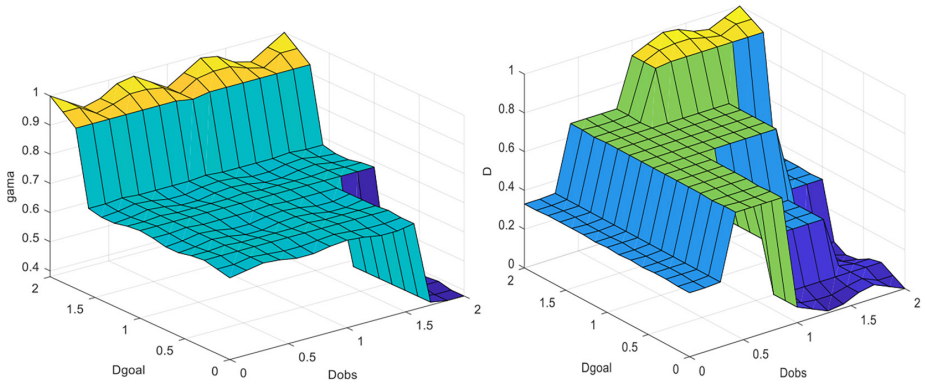

(c) γ output (d) λ output

Figure 3. Output membership function

nodes. The fused algorithm is shown in Figure 4. On the premise of ensuring the global optimum, this integrated approach not only efficiently navigates around moving obstacles but also prevents unnecessary path meandering, so as to achieve an ideal smooth path, which is more conducive to the later path tracking.

RESULTS

Simulation analysis and experimental verification

To assess the practicality and efficiency of the enhanced fusion algorithm, a series of simulations are carried out on relevant software platforms. The simulation process is divided into 2 parts. One part is to validate the feasibility and practicability of the enhanced A * algorithm, and the other part is to verify the adaptability and practicality of the enhanced fusion algorithm. In this study, the grid method is used to construct the experimental simulation environment. To enhance the efficiency of simulation and simplify the expression of irregular obstacles and path slopes in the simulation map environment, the following two assumptions are made. Firstly, the height and shape information of obstacles are ignored in the simulation map, and the non-horizontal areas are replaced by their projected ground areas. Secondly, when AGV moves on the non-horizontal plane, the slope angle and the tilt angle are the same.

Simulation result of enhanced A algorithm*

In order to assess the performance of the enhanced A* algorithm, path planning simulation experiments are conducted on 20 × 20, 25 × 25, 30 × 30, 35 × 35 and 40 × 40 two-dimensional grid maps respectively, with comparisons made against the conventional A* algorithm. The results of these simulation experiments are presented in Figure 5 and Table 2.

From the results of the simulation experiments, it can be concluded that in terms of the planned path distance, the enhanced A* algorithm is slightly superior to the conventional A* algorithm, which gains a shorter path and runs more smoothly. In terms of running time, the enhanced A* algorithm has achieved a significant enhance compared with the conventional A* algorithm, with its running time reduced by more than half. The corresponding running times of the 20 × 20, 25 × 25, 30 × 30,

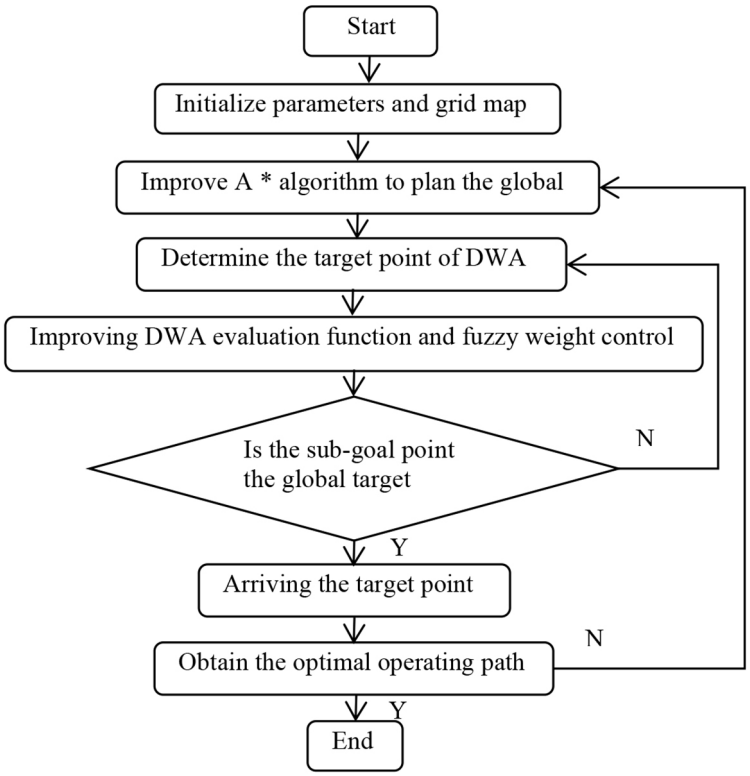

Figure 4. Workflow of the enhanced fusion algorithm

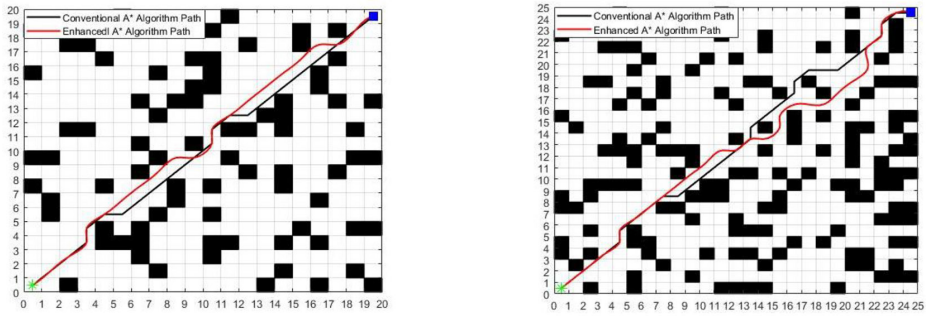

(a) 20×20Map　　(b) 25×25Map

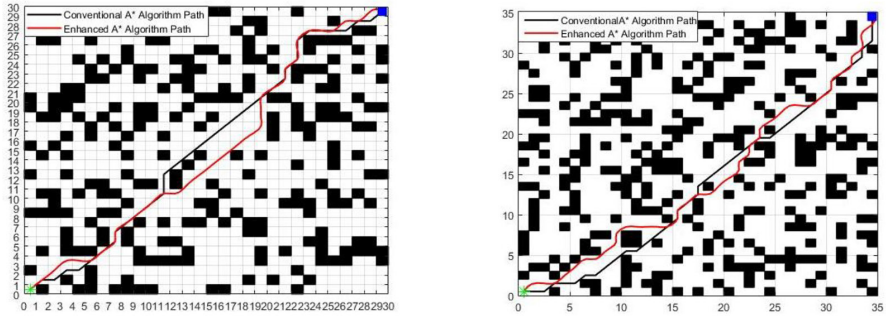

(c) 30×30Map　　(d) 35×35Map

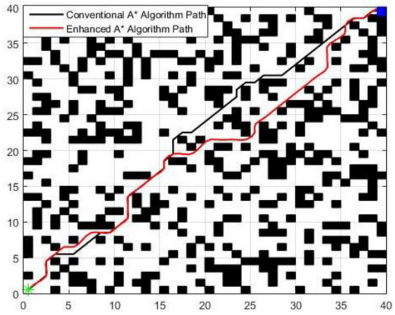

(e) 40×40 Map

Figure 5. Comparison of the path planning between enhanced A* and conventional A*

Table 2. Comparison of performance data between enhanced A *and conventional A *(Mean±Std over 15 runs)

Map	Algorithm	Path distance/m	Runtime/s
20 × 20	conventional A *	28.342±0.052	0.071±0.005
	enhanced A *	28.013±0.045	0.035±0.003
25 × 25	conventional A *	36.871±0.061	0.081±0.002
	enhanced A *	36.293±0.059	0.037±0.004
30 × 30	conventional A *	45.412±0.075	0.161±0.005
	enhanced A *	44.526±0.067	0.059±0.003
35 × 35	conventional A *	53.942±0.083	0.183±0.006
	enhanced A *	52.583±0.079	0.053±0.003
40 × 40	conventional A *	61.598±0.103	0.378±0.011
	enhanced A *	60.426±0.096	0.126±0.003

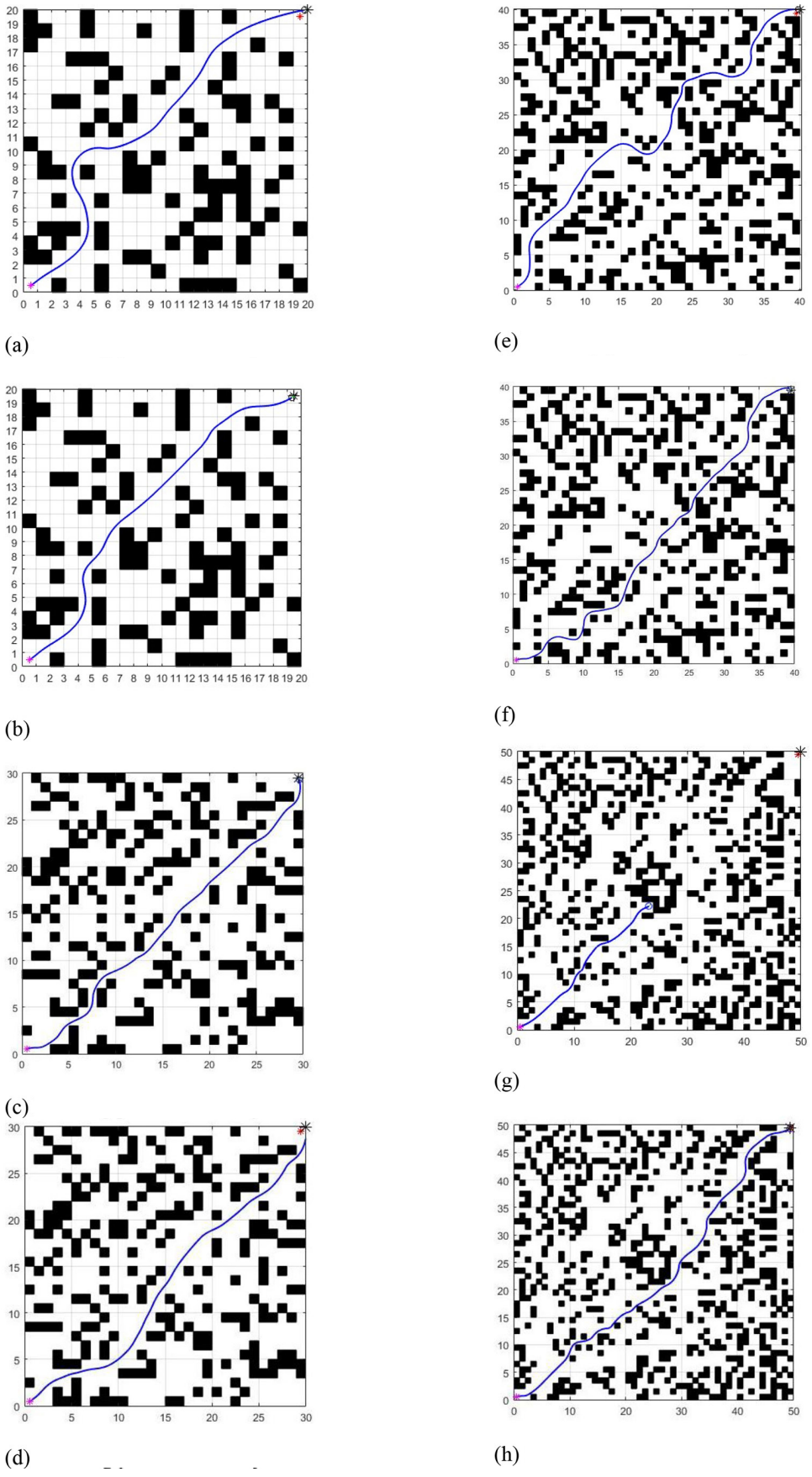

Figure 6. Comparison of path planning for different fusion algorithms (a) planning path obtained by the conventional fusion algorithm for a 20×20 map, and (b) by the enhanced fusion algorithm for a 20×20 map, (c) planning path obtained by the conventional fusion algorithm for a 30×30 map, and (d) by the enhanced fusion algorithm for a 30×30 map, (e) planning path obtained by the conventional fusion algorithm for a 40×40 grid map, and (f) by the enhanced fusion algorithm for a 40×40 map, (g) planning path obtained by the conventional fusion algorithm for a 50×50 map, and (h) by the enhanced fusion algorithm for a 50×50 map

35 × 35, and 40 × 40 grid maps are saved by 50.71%, 54.32%, 63.35%, 71.04% and 66.67% respectively. Therefore, the running speed and efficiency of the algorithm can be significantly enhanced without obviously affecting the quality of the path through introducing the weight factor and smoothing processing.

Simulation comparison of the enhanced fusion algorithm

To test the effectiveness and stability of the enhanced fusion algorithm, four kinds of grid maps, which include 20 × 20, 30 × 30, 40 × 40 and 50 × 50, were established for simulation analysis. The results of these simulation experiments are presented in Figure 7 and Table 3.

The simulation results in Figure 6 and Table 3 indicate that the enhanced fusion algorithm demonstrates superior overall performance in the path planning compared to that in the conventional fusion algorithm. When evaluating the path distance, the enhanced algorithm generates shorter paths, which obtain reductions of approximately 9.18% in the 20 × 20 map, 4.45% in the 30 × 30 map, and 6.26% in the 40 × 40 map. In terms of path smoothness, the enhanced fusion algorithm outperforms the conventional fusion algorithm in two indicators, namely the count of turning points and the cumulative turning angle with particularly superior performance in the 30 × 30 map, where these metrics decreased by 70.3% and 74.93% respectively. In runtime performance, the enhanced fusion algorithm exhibits shorter computation time and higher search efficiency. Concerning algorithmic adaptability, the search capability and adaptability of the conventional fusion algorithm gradually decline as the map complexity increases. Particularly in the 50 × 50 map, it demonstrates inefficient search capability and fails to find an optimal solution. In contrast, the enhanced fusion algorithm maintains the ability to identify the optimal paths in the complex environments.

Overall, contrasted with conventional fusion algorithms, the enhanced fusion algorithm is closer to the global energy-saving path, which can effectively reduce the loss of additional energy, adaptively adjust the heading angle, reduce redundant steering, make the trajectory smoother, and enhancing the exploration efficiency and planning effect of AGV in the navigation process.

Testing and verification

To further verify the reliability and practicability of the enhanced fusion algorithm in the actual application, the enhanced fusion algorithm is applied to AGV for the material distribution in an automatic welding workshop. AGV is a load type and it uses a SLAM laser for navigation. Meanwhile, the navigation accuracy is ± 10 mm, the parking accuracy is ± 5 mm, and the driving speed is 10 m/min. Its form is shown in Figure 7.

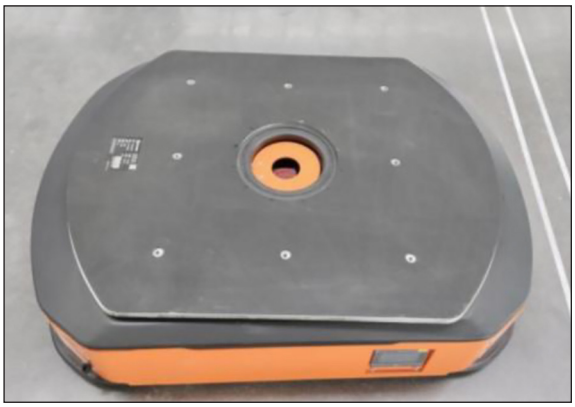

Figure 7. Load-bearing AGV

Table 3. Simulation experiment data of different fusion algorithms(Mean±Std over 15 runs)

Map	Algorithm	Path distance /m	Turning points	Cumulative turning angle °	Runtime /s
20 × 20	Conventional fusion algorithm	31.252±0.13	101±2.3	148.7±3.4	212.263±4.3
	Enhanced fusion algorithm	28.384±0.11	94±1.8	136±3.2	182.846±3.8
30 × 30	Conventional fusion algorithm	43.541±0.21	165±4.2	216.6±5.3	522.841±9.8
	Enhanced fusion algorithm	40.607±0.18	49±2.3	54.3±2.3	490.461±8.6
40 × 40	Conventional fusion algorithm	64.282±0.28	327±6.5	500.9±8.6	1001.513±13.6
	Enhanced fusion algorithm	60.259±0.23	260±5.8	360±7.3	790.816±12.9
50 × 50	Conventional fusion algorithm	/	/	/	/
	Enhanced fusion algorithm	73.113±0.35	248±6.7	356.7±10.1	151.388±7.8

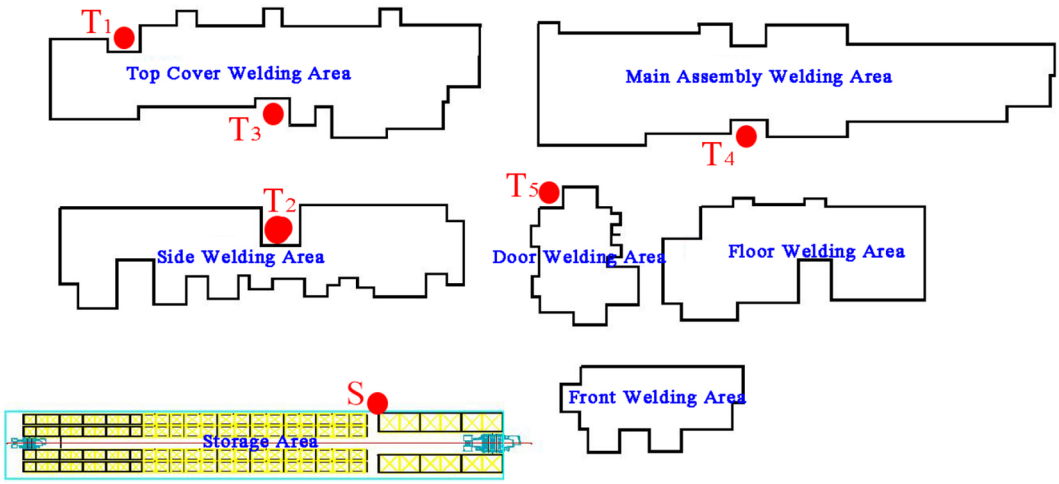

Figure 8. Layout plan of an automatic welding workshop

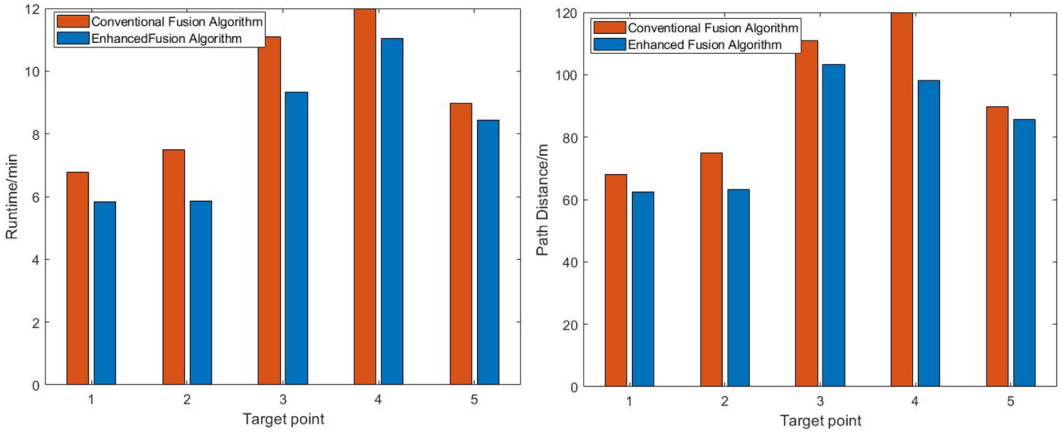

(a) Running time (b) Distances of planned path

Figure 9. Test data of conventional fusion algorithm and enhanced fusion algorithm

The experimental verification is carried out in an automatic welding workshop, and the layout of the workshop is shown in Figure 8. Starting from the point S in the material area, AGV delivers these materials to five target points (T_1~T_5) respectively. Experiments on dynamic path planning for AGV were conducted using both conventional fusion algorithms and enhanced fusion algorithms, respectively. Repeated experiments are carried out and the test data are documented in Figure 9. Analyzing the recorded test data from Figure 9 reveals that the enhanced fusion algorithm outperforms the conventional fusion algorithm in both path planning quality and operational efficiency, and is consistent with the simulation results, which demonstrates the practicality and effectiveness of the enhanced algorithm.

CONCLUSIONS

To enhance the path planning performance and efficiency of AGV in the complex environment, a fusion algorithm combining enhanced A* and enhanced DWA was presented. The algorithm successfully addressed the limitations of the conventional A* algorithm, such as inefficient searching processes, unsmooth path, and the redundancy of the DWA algorithm, which is easy to fall into the suboptimal solution. Through experimental verification, the following conclusions are gained.

The conventional A* algorithm was enhanced by introducing weight factors and adopting cubic B-spline curves. Compared with the conventional A* algorithm, the enhanced A* algorithm reduced the path distance by approximately 1.82% and the

running time by 61.24% on average, effectively improving the overall path planning efficiency.

By incorporating distance correction function and fuzzy weight control, the robustness and stability of the DWA algorithm were enhanced. The enhanced DWA algorithm was then fused with the enhanced A* algorithm to gain the enhanced fusion algorithm. Compared to the conventional fusion algorithm, the proposed enhanced fusion algorithm demonstrated higher search efficiency and stronger adaptability in complex environments. For instance, when tested on a 30 × 30 grid environment, this method achieved a 4.45% reduction in path length, a 6.12% decrease in execution time, a 70.3% reduction in the count of turning points, and a 74.93% minimization of cumulative turning angles. All test results indicate that the enhanced fusion algorithm generated smoother paths, ensured the global optimality, and exhibited superior adaptability to the complex environments with higher operational efficiency.

The proposed algorithm was developed and validated under the following assumptions: a) The environment was modeled as a 2D grid map, where vertical obstacles and terrain elevation were neglected. b) Obstacles were treated as static during global path planning, while their movements were assumed to be linearly predictable in local dynamic planning. c) AGV adhered to a differential drive kinematic model with no slippage. d) Map boundaries and global static obstacles were assumed to be a priori known. In real-world scenarios involving unknown environments, severe sensor degradation, or highly nonlinear dynamic obstacles, supplementary modules for robust perception, uncertainty mitigation, and real-time map updating will be indispensable. Future research will focus on integrating real-time sensor fusion, 3D environment modeling, and learning-based dynamic obstacle prediction to extend the applicability of the algorithm to more unstructured and uncertain contexts.

REFERENCES

1. Wang R., Wang Z T., Ding J. Path planning for mobile robot based on improved ant colony algorithm. Applied Mechanics and Materials. 2013, 717–720. https://doi.org/10.4028/www.scientific.net/AMM.385-386.717
2. Liu Y., Hu L., Ma Z. A new adaptive differential evolution algorithm fused with multiple strategies for robot path planning. Arab J Sci Eng.2024, 49, 11907–11924. https://doi.org/10.1007/s13369-023-08380-w
3. Gu C C., Liu S Y., Li H S. Research on hybrid path planning of underground degraded environment inspection robot based on improved A* algorithm and DWA algorithm. Robotica. 2025, 43, 1–22. https://doi.org/10.1017/S0263574725000037
4. Öztürk Ü., Akdağ M., Ayabakan T. A review of path planning algorithms in maritime autonomous surface ships: Navigation safety perspective. Ocean Engineering. 2022, 254, 111010. https://doi.org/10.1016/j.oceaneng.2022.111010
5. Guan C X., Zhang S Y. Robot dynamic path planning based on improved A* and DWA algorithms. International Conference on Control and Robotics. 2022, 1–6. https://doi.org/110.1109/ICCR55715.2022.10053929
6. Li C Y., Yao L., Mi C. Fusion algorithm based on improved A* and DWA for USV path planning. Journal of Marine Science and Application. 2025, 24, 224–237. https://doi.org/10.1007/s11804-024-00434-1
7. Zhen Y., Li J L. A smooth jump point search algorithm for mobile robots path planning based on a two-dimensional grid model. Journal of Robotics. 2022, 1–15.https://doi.org/10.1155/2022/7682201
8. Guo T., Sun Y Q., Liu Y. An automated guided vehicle path planning algorithm based on improved A* and dynamic window approach fusion. Applied Sciences (Switzerland). 2023, 13, 10326. https://doi.org/10.3390/app131810326
9. Vagale A., Oucheikh R., Bye RT. Path planning and collision avoidance for autonomous surface vehicles I: a review. Journal of Marine Science and Technology. 2021, 26, 1292–1306. https://doi.org/10.1016/j.oceaneng.2022.111010
10. Yin X., Cai P., Zhao K. Dynamic path planning of AGV based on kinematical constraint A* algorithm and following DWA fusion algorithms. Sensors. 2023, 29, 4102. https://doi.org/10.3390/s23084102
11. Sabag J., Pinkovich B., Rivlin E. Efficient coverage path planning for a drone in an urban environment. Drones. 2025, 9, 98. https://doi.org/10.3390/drones9020098
12. Li Y B., Wang Z X., Zhang S Y., Path Planning of Robots Based on an Improved A-star Algorithm. 2022 IEEE 5th Advanced Information Management, Communicates, Electronic and Automation Control Conference (IMCEC), Chongqing, China, 2022, 826–931. https://doi.org/10.1109/IMCEC55388.2022.10019799
13. Luo Z.,Han Y., Zhang X., Zou Y. Research on path planning of inspection robot with improved RRT-connect and DWA algorithm. Computer Engineering and Applications. 2024, 60, 344–354. https://doi.org/10.3778/j.issn.1002-8331.2312-0213

14. Cao L L., Tang L., Cao S Q. Smooth optimised A*-Guided DWA for mobile robot path planning. Applied Sciences. 2025, 15, 6956. https://doi.org/10.3390/app15136956
15. Vikas., Dayal R. P. Multi-robot path planning using a hybrid dynamic window approach and modified chaotic neural oscillator-based hyperbolic gravitational search algorithm in a complex terrain. Intelligent Service Robotics. 2023, 16, 213–230. https://doi.org/10.6041/j.issn.1000-1298.2021.01. 002
16. Li P Y., Hao L J., Zhao Y J. Robot obstacle avoidance optimization by A* and DWA fusion algorithm. PloS one. 2024, 19, e0302026. https://doi.org/10.1371/journal.pone.0302026
17. Wei G A., Zhang J Q. Research on unmanned surface vessel aggregation formation based on improved A* and dynamic window approach fusion algorithm. Applied Sciences. 2023, 13, 8625. https://doi.org/10.3390/app13158625
18. Daniela Teso-Fz-Betoño., Iñigoa A., Jose Antonioa. Optimization of energy efficiency with a predictive dynamic window approach for mobile robot navigation. Sustainability. 2025, 17, 4526. https://doi.org/10.3390/su17104526
19. Lai R S., Wu Z Y., Liu X G., Zeng N Y. Fusion algorithm of the improved A* algorithm and segmented Bézier curves for the path planning of mobile robots. Sustainability. 2023, 15, 2483. https://doi.org/10.3390/su15032483
20. Nowakowski M. Operational Environment Impact on Sensor Capabilities in Special Purpose Unmanned Ground Vehicles.2024 21st International Conference on Mechatronics - Mechatronika (ME), Brno, Czech Republic. 2024, 1–5. https://doi.org/10.1109/ME61309.2024.10789716
21. Aizat M., Qistina N., Rahiman W. A Comprehensive Review of Recent Advances in Automated Guided Vehicle Technologies: Dynamic Obstacle Avoidance in Complex Environment Toward Autonomous Capability. IEEE Transactions on Instrumentation and Measurement. 2024, 73, 1–25. https://doi.org/10.1109/TIM.2023.3338722
22. Liu L S., Yao J X.,He D W., Global dynamic path planning fusion algorithm combining jump-A* algorithm and dynamic window approach. IEEE Access. 2021, 9, 19632–19638. https://doi.org/10.1109/ACCESS.2021.3052865
23. Chang Z., Zhang Z., Yang M. Improved dynamic path planning algorithm of mobile robot based on fusion of A* and DWA. Advances in Mechanical Design. 2024, 569–584. https://doi.org/10.1007/978-981-97-0922-9_37
24. Su C., Zhao L L., Xiang D B. Adaptive A*–Q-Learning–DWA fusion with dynamic heuristic adjustment for safe path planning in spraying robots. Applied Sciences. 2025, 15, 9340. https://doi.org/10.3390/app15179340
25. Liu Y., Li C H., Wang Q T. Adaptive dynamic windowing approach based on risk degree function.Transactions of the Institute of Measurement and Control. 2024, 46, 1542–1550. https://doi.org/10.1177/014233122311998071
26. Guo H P., Li Y., Wang H., Wang C S. Path planning of greenhouse electric crawler tractor based on the improved A* and DWA algorithms. Computers and Electronics in Agriculture.2024, 227, 109596. https://doi.org/10.1016/j.compag.2024.109596
27. Xie Y S., Liu C Y., He Y X., Ma Y. Multi-strategy fusion path planning algorithm for autonomous surface vessels with dynamic obstacles. Journal of Marine Science and Engineering.2025, 137, 1357. https://doi.org/10.3390/jmse13071357